Original Research

Extracellular polymeric substances as paper coating biomaterials derived from anaerobic granular sludge

Cuijie Feng [a, b, *], Lorenzo Bonetti [c], Hui Lu [d], Zhongbo Zhou [e], Tommaso Lotti [f], Mingsheng Jia [g], Giacomo Rizzardi [a], Luigi De Nardo [c], Francesca Malpei [a]

[a] Department of Civil and Environmental Engineering, Politecnico di Milano, Piazza Leonardo da Vinci, 32, 20133, Milan, Italy
[b] School of Civil Engineering, Sun Yat-sen University, 519082, Zhuhai, China
[c] Department of Chemistry, Materials and Chemical Engineering "G. Natta", Politecnico di Milano, Via Mancinelli, 7, 20131, Milan, Italy
[d] School of Environmental Science and Engineering, Sun Yat-sen University, 510275, Guangzhou, China
[e] Southwest University, College of Resources and Environment, Tiansheng Road 2, Beibei District, 400716, Chongqing, China
[f] Civil and Environmental Engineering Department, University of Florence, Via di Santa Marta 3, 50139, Florence, Italy
[g] Center for Microbial Ecological and Technology (CMET), Ghent University, Coupure Links 653, Gent, Belgium

ARTICLE INFO

ABSTRACT

Recovering extracellular polymeric substances (EPS) from waste granular sludge offers a cost-effective and sustainable approach for transforming wastewater resources into industrially valuable products. Yet, the application potential of these EPS in real-world scenarios, particularly in paper manufacturing, remains underexplored. Here we show the feasibility of EPS-based biomaterials, derived from anaerobic granular sludges, as novel coating agents in paper production. We systematically characterised the rheological properties of various EPS-based suspensions. When applied as surface sizing agents, these EPS-based biomaterials formed a distinct, ultra-thin layer on paper, as evidenced by scanning electron microscopy. A comprehensive evaluation of water and oil penetration, along with barrier properties, revealed that EPS-enhanced coatings markedly diminished water absorption while significantly bolstering oil and grease resistance. Optimal performance was observed in EPS variants with elevated protein and hydrophobic contents, correlating with their superior rheological characteristics. The enhanced water-barrier and grease resistance of EPS-coated paper can be attributed to its non-porous, fine surface structure and the functional groups in EPS, particularly the high protein content and hydrophobic humic-like substances. This research marks the first demonstration of utilizing EPS from anaerobic granular sludge as paper-coating biomaterials, bridging a critical knowledge gap in the sustainable use of biopolymers in industrial applications.

© 2024 The Authors. Published by Elsevier B.V. on behalf of Chinese Society for Environmental Sciences, Harbin Institute of Technology, Chinese Research Academy of Environmental Sciences. This is an open access article under the CC BY-NC-ND license (http://creativecommons.org/licenses/by-nc-nd/4.0/).

1. Introduction

Biological treatment based on activated sludge has been the most widely used approach in removing major pollutants from wastewater. However, excess sludge disposal accounts for up to 50% of total wastewater treatment costs and presents a significant challenge in wastewater treatment [1]. To address this issue, wastewater treatment plants (WWTPs) are shifting from merely removing pollutants to recovering raw materials, turning themselves into potential renewable sources [2,3]. Thus, resource recovery from excess sludge, rich in extracellular polymeric substance (EPS), is becoming increasingly attractive and contributes to implementing the "biorefinery" paradigm from wastewater treatment plants [3–5]. EPS-based biomaterials are potential alternatives to synthetic polymers in various applications, such as agriculture, medical, and construction industries, as they have polysaccharides (PS), proteins (PN), and humic-acid substances [6]. Recent years have increased our understanding and development of EPS-based biomaterials for different applications, including environmental pollution control, industrial/agricultural trials, and achieving resource recovery while promoting a circular economy [3].

* Corresponding author. Department of Civil and Environmental Engineering, Politecnico di Milano, Piazza Leonardo da Vinci, 32, 20133, Milan, Italy.
E-mail address: fengcj@mail.sysu.edu.cn (C. Feng).

Nomenclature		EEM	Excitation-emission matrix
		Em	Emission wavelengths
AnGS	Anaerobic granular sludge	Ex	Excitation wavelength
AGS	Aerobic granular sludge	$F_{lg}(d_i)$	The cumulative probability function
AnGS-B	Anaerobic granules collected from a brewery wastewater treatment plant	MW	Molecular weight
		PN	Proteins
AnGS-P	Anaerobic granules taken from a paper-industry wastewater treatment plant	PS	Polysaccharides
		PN/PS	The protein to polysaccharide ratio
ATR-FTIR	Attenuated total reflectance-fourier transform infrared spectra	PSD	Particle size distribution
		SRD	Surface repellency degree
d_i	The average diameter of the single-particle size class	TSS	Total suspended solids
$f_i(d_i)$	The frequency of the particle size class	VSS	Volatile suspended solids
$f_{lg}(d_i)$	The probability density function	WWTP	Wastewater treatment plant
EPS	Extracellular polymeric substance	WA	Water absorbance

Specifically, EPS-based biomaterials have shown potential in various uses, such as flame-retardant materials [7] and concrete curing agents [3]. As for paper coating, the demand for paper and paperboard production continuously grows worldwide, particularly in the packaging industry [8], which accounts for the largest share of global paper production (over 33%). Nevertheless, due to the paper's nature and dependence on the application, it usually requires surface coating to achieve barrier properties. With rising environmental concerns, using renewable coating materials can support sustainability strategies.

This study examines the potential of EPS-based biomaterials from anaerobic granular sludges for paper coating. Previous studies have demonstrated that EPS recovered from aerobic granules has desirable film-forming properties attributed to amphiphilic properties due to the PS and lipid composition [9]. However, very few studies have compared EPS barrier properties. It is unclear whether EPS-based biomaterials from different sources of granular sludges display similar properties. More research is needed to reveal the underlying water barrier mechanism of EPS-coated paper due to the complex and diverse composition of EPS. Designers and marketers should consider the environmental impact of packaging at the early stage of production, particularly given the rising demand in the packaging industry, and minimise costs and environmental impacts.

Many studies have focused on producing and applying EPS-based biomaterials from aerobic granular sludge (AGS) by recovering bioplastics, phosphate, and alginate-like extracellular biopolymers [10]. To date, nearly 100 full-scale AGS systems have been installed worldwide [11]. The corresponding EPS contents in AGS are of the order of 38−372 mg EPS per g of volatile suspended solids (VSS) and slightly lower (60−290 mg EPS per g VSS) in anaerobic granular sludge (AnGS) [6]. Despite the wide presence of AnGS-based installations biodegrading large amounts of industrial wastewater, limited attention has been given to the recovery and application of EPS from AnGS [12]. A better understanding of the yield and properties of EPS derived from AnGS is essential to maximise resource recovery and successfully design and manage future biorefinery implementations. The composition, yield, and properties of EPS vary depending on the source of granular sludge, which is closely associated with downstream applications of EPS-based biomaterials. Thus, a comprehensive evaluation of these biomaterials' physicochemical properties, yield, and quality is necessary. Such understanding can improve the development of anaerobic systems and help devise effective strategies for resource recovery and biofilm control in WWTPs. This study aims to shed light on the potential of AnGS in terms of resource recovery.

To investigate the impact of anaerobic granule origin on EPS properties and application of EPS-based biomaterials, this study focused on three key points: (1) Differences in EPS characteristics between different kinds of anaerobic granules; (2) Their impact on the EPS coating's behaviour and effectiveness; (3) Components in EPS that are the key indicator for the desired paper coating properties. We selected two typical granules from full-scale industrial WWTPs to achieve these goals. Analysing granules from full-scale WWTPs instead of lab-scale sources proved more representative and beneficial for evaluating sustainable EPS biomaterials. Understanding these differences in EPS characteristics and the EPS production process's optimisation is crucial for recovering EPS as biomaterials for the paper industry. The results of this study contribute significantly to the biorefinery approach of EPS-based biomaterials, particularly in terms of paper coating applications.

2. Materials and methods

2.1. Sampling and sludge characterisation

Anaerobic granules were collected from a brewery wastewater treatment plant (AnGS-B) and a paper-industry wastewater treatment plant (AnGS-P). Total suspended solids (TSS) and VSS were measured using standard methods [13], and the granule size was quantitatively compared using ImageJ software. Over ten sample images were analysed for particle size distribution (PSD) analysis. The parameters analysed were the number and particle area in each image. Starting from dimensional data, a log-normal distribution was used to plot the grain size curve [14]. The average granule diameter (D_{av}) was calculated from the average diameters of all classes and the detection frequencies (equation (1)). Afterwards, the log-normal curve parameters of mean (μ) and variance (σ^2) were calculated using equations (2) and (3). The probability density function (equation (4)) and the cumulative distribution function (equation (5)) were estimated as follows:

$$D_{av} = \frac{\sum\limits_{i=1}^{n} d_i \times f_i(d_i)}{\sum\limits_{i=1}^{n} f_i(d_i)} \tag{1}$$

$$\mu = \ln D_{av} = \sum_{i=1}^{n} \ln(d_i) \times f_i(d_i) \tag{2}$$

$$\sigma^2 = \sum_{i=1}^{n} [\ln(d_i) \times \ln(D_{av})]^2 \times (d_i) \tag{3}$$

$$f_{lg}(d_i) = \frac{1}{D_{av}\sigma\sqrt{2\pi}} \exp\left\{-\frac{1}{2}\left[\frac{\ln(D_{av}) - \mu}{\sigma}\right]\right\} \tag{4}$$

$$F_{lg}(d_i) = \int_0^{d_i} \frac{1}{D_{av}\sigma\sqrt{2\pi}} \exp\left\{-\frac{1}{2}\left[\frac{\ln(D_{av}) - \mu}{\sigma}\right]\right\} d(d_i) \tag{5}$$

where d_i indicates the average diameter of the single-particle size class, $f_i(d_i)$ stands for the frequency of the particle size class, $f_{lg}(d_i)$ is the probability density function, and $F_{lg}(d_i)$ denotes the cumulative probability function.

2.2. EPS extraction and biopolymer fractional size distribution analysis

According to previous studies, EPS were extracted from granules using the Na_2CO_3-heating method [15]. Briefly, Na_2CO_3 was added to improve the extraction efficiency with a final concentration of 0.5% (weight, wt). Na_2CO_3 and granular sludge mixture was heated at 80 °C for 30 min. Applying a centrifugal filter device with membrane (CFDM) resulted in a much shorter time required for the extraction process. The CFDM with different membrane sizes (3, 30, and 100 kDa) was used to study the biopolymer size distribution behaviour.

2.3. Chemical properties of EPS

The EPS yield is defined as the VSS fraction of EPS extracts per unit of the VSS of pristine granules. The PS fraction was measured using the phenol-sulphuric acid method with glucose as the standard [16]. The PN content was determined using the bicinchoninic acid assay kit with Bovine Serum Albumin as the standard (B9643, Sigma Aldrich, Merck, Germany) [17]. The EPS yield, PN, and PS were always referred to VSS contents in initial dry granules.

2.4. Spectroscopic analysis

An excitation-emission matrix (EEM) fluorescence spectroscopy analysis of EPS aquatic samples was performed using luminescence spectrometry (Cary Eclipse, Agilent, USA). EEM spectra were scanned with emission wavelengths (Em) from 300 to 550 nm at 0.5 nm increments by varying the excitation wavelength (Ex) from 220 to 400 nm (10 nm increments). Excitation and emission slits were maintained at 10 nm. The scan speed was set at 1200 nm min^{-1} for all measurements. To reduce potential interference, EPS samples at 3 kDa from Section 2.2 were used for the EEM analysis. Ultrapure water was used as a blank. EEM spectra were illustrated as the elliptical shape of contours using MatLab 6.5 (MathWorks Inc., USA). The functional groups of EPS solutions were detected by Attenuated Total Reflectance-Fourier Transform InfraRed spectra (ATR-FTIR, Varian 640, USA) with a 4000 and 500 cm^{-1} scan range.

2.5. Rheological behaviour tests on EPS extracts

Rheological properties of EPS specimens were tested using a rotational rheometer (MCR302 Anton Paar) equipped with a plate-plate geometry ($\varphi = 25$ mm) and a working gap of 0.4 mm. First, strain sweep measurements were carried out to identify the linear viscoelastic region (LVE) of each specimen, applying an oscillatory strain (γ) in the 0.01−100% strain range at T = 25 °C and frequency

(ν) = 1 Hz. Before each measurement, a 1-min pre-conditioning step (T = 25 °C, γ = 0.01%, ν = 1 Hz) was carried out to ensure the homogeneity of the EPS solutions. Then, frequency sweep tests were performed in the 0.01−100 Hz frequency range at γ = 0.2% (i.e., the limit of the LVE region). Before each measurement, a 1 min pre-conditioning step (T = 25 °C, γ = 0.2%, ν = 0.01 Hz) was carried out to ensure the homogeneity of the EPS solutions.

2.6. Scanning electron microscopy (SEM) observation

EPS pellets were centrifuged using CFDM at 3 kDa and then lyophilised by a vacuum freeze dryer (ScanVac Coolsafe, LaboGene, Denmark) at −50 °C for 48 h. Then lyophilised EPS extracts and paper were observed using SEM Zeiss EVO 50 EP with Spectrometer EDS Bruker Quantax 2006/30.

2.7. Waterproofing and grease resistance tests

A commercial coating agent - carboxymethyl cellulose (CMC, Sigma Aldrich), was used as a reference product in the paper industry. CMC is an anionic cellulose derivative obtained by introducing carboxymethyl groups along the cellulose chain [18,19]. CMC has been used in different industries, such as textile and food. The coating solution applied on paper was first prepared by mixing EPS with a final fraction of 8% (w/v) and CMC with a final fraction of 9% (w/v). The solution's pH was adjusted to 8.0. As shown in Fig. 1, coatings were prepared using the Sheen 1137 automatic film applicator and the Meyer 1120/25/76 bar at 100 mm s^{-1}. A mixed solution (3 mL) containing 8% EPS and 9% CMC for each coating was homogeneously spread over a sheet of paper with a weight density equal to 37.9 g cm^{-2}. After spreading, each sheet was immediately transferred to a ventilated oven and dried for 5 min at 80 °C. The sheets were subsequently stored in a room conditioned at 23 °C. The water absorbance capacity was measured using the Cobb method (UNI EN ISO 535). The surface wettability was analysed by the evolution over time and the droplet volume (ATICELCA MC 21−72). The resistance to grease, oil and waxes was evaluated by measuring permeability (turpentine oil method, ISO 16532-1:2010) and surface repellence (ISO 16532-2:2010).

3. Results and discussion

3.1. General characteristics of the anaerobic granules

Differences in morphology were observed in colour, particle size, and VSS content (Fig. 2). As shown in Fig. 2a and b, the colour
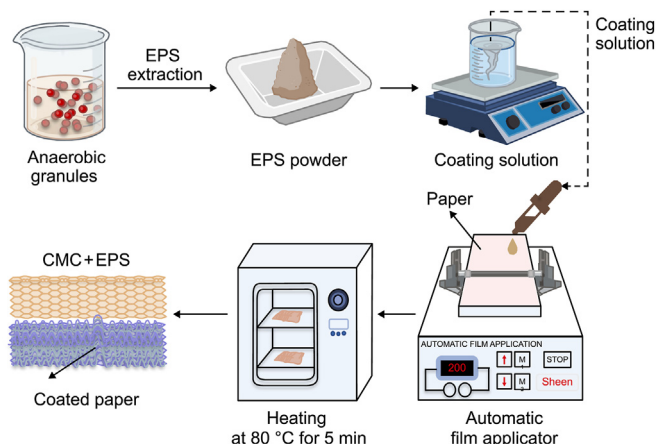

Fig. 1. Paper coating process using EPS-based biomaterials.

of anaerobic granules was brown or black with a smooth surface. Fig. 2c and d represent particle size distribution for the two granule types. Patterns of size distribution curves for all samples were quite similar, typically presenting one peak. However, there are comparative differences, particularly in mean diameter values. The dimension of AnGS-P granules was larger, with an average diameter of about 3.5 mm. The AnGS-B samples were mostly 2.3 mm in diameter, with a small number of very large granules (up to 8 mm).

From the calculated values and the comparison between the different curves (Fig. 2e—Table 1), a similar pattern was observed in other anaerobic brewery granules reported elsewhere [20]. The AnGS-P granules had a very wide size distribution, suggesting a more homogeneous distribution of granule diameter sizes than the other samples. Also, the analysis of the composition of the granules was performed based on an ash fraction calculation together with TSS and VSS measurements. According to Fig. 2f, the VSS fractions of AnGS-B and AnGS-P took the fractions within 93% and 83% of TSS, respectively.

3.2. EPS yield and component characterisation

Fig. 3a presents the variations in EPS content, compositions, and the PN/PS ratio of EPS extracts from AnGS. The AnGS-P had a higher EPS yield, with 408 ± 16 mg per g VSS, compared to 360 ± 17 mg per g VSS from the AnGS. The EPS contents displayed fractions of 36−41% in VSS of the original granules, in line with previous studies [15,21]. Intensive studies have pointed out PN and PS as the main contents of EPS. Similarly, in this study, the relative abundance of PN and PS was above 62%. The characteristics of granules are related to the PN/PS ratio, which indicates the granule's stability, compactness, and hydrophobicity [22]. High PN contents in EPS can

enhance the stability of granules [23]. More precisely, between the different samples, the PS amounts were in the range of 51−71 mg per g VSS. The fractions of the PN contents accounted for 49−59% of the EPS. For the AnGS-P sample, protein contents took the largest fractions of over 59% in EPS, followed by PS with 17%; for the AnGS-B sample, the percentages of protein and PS normalised to EPS were 17% and 14%, respectively. Therefore, it is clear that more contents were detected in the AnGS-P samples.

The molecular size distribution of EPS contents is one of the most important characteristics. Sizes of biopolymers in EPS products have shown a broad distribution [15,24]. The biopolymer fractional size distribution of extractable EPS products from these granules was studied using centrifugal filtering devices with different cut-offs of 3, 30, and 100 kDa to further understand size-fractionated molecules in EPS. According to this information, four categories can be defined based on the molecular weight (MW): small (<3 kDa), low (3−30 kDa), medium (30−100 kDa), large (>100 kDa) [15]. For PS, all the EPS with MW over 30 kDa dominated, ranging from 63 to 78%, indicating the presence of long-chain PS, with the dimension of most of them being >100 kDa (from 51% to 65%, Fig. 3b). Similarly, protein MW distribution in EPS showed major long-chain molecules with MW over 3 kDa, within the 62−72% range, which was in line with previous studies [15]. Therefore, the fraction of short-chain PN varied between 29% and 40%. Similarly, the PN fraction with medium MW is the least abundant of the four classes. From biopolymer size distribution analysis, we inferred no significant differences between the EPS extracted regardless of the different types of granular sludges, and the size of PN and PS may not be significantly affected by the operating conditions or wastewater composition.

3.3. Spectral characteristics of EPS and protein secondary structure analysis

ATR-FTIR spectroscopy was carried out to investigate the functional groups of EPS obtained from granular sludge samples (Fig. 4a). No differences in the positions and number of peaks were detected for the EPS specimens, indicating a similar nature of the chemical groups present in the EPS fractions. Several frequency bands associated with PN and PS were detectable in the EPS spectra [15]. In particular, the bands at 3500−3100 cm^{-1} were attributed to the O−H stretching vibration of hydroxyl compounds and N−H stretching vibration (PN, peptides). Other predominant bands were as follows: 2937 cm^{-1} (C−H stretching vibration) reflecting alkyl chains, 1650 cm^{-1} (Amide I), 1560 cm^{-1} (Amide II), 1250 cm^{-1} (Amide III) referred to PN, and 1080 cm^{-1} assigned to the C−O−C stretching vibration absorption peak of hydroxyl in PS [25−27]. The band at 1402 cm^{-1} was attributed to the symmetric stretching vibration of deprotonated carboxylic acid groups, unveiling the acidic nature of EPS components [26]. The peak intensities of the two EPS samples were significantly different, with higher indications of EPS samples from AnGS-P [26].

Given the significance of the secondary structure of extracellular PN in granule properties (e.g., hydrophobicity) and mechanical properties [28], the amide I region (1700−1600 cm^{-1}) was further resolved into secondary protein structures spectra through the second derivative analysis and curve fitting program. Secondary structures, α-helix, β-sheet, β-turn, and random coil, were assigned according to values reported elsewhere in the literature [29]. As shown in Fig. 4b and c, the EPS extracted from AnGS-P had eight bands, four β-sheet bands, one α-helix band, one β-turn band, and two random bands, that extracted by AnGS-B had two β-sheet bands, two α-helix bands, one β-turn band, and one random band. The above findings indicate that the different granular sludge sources' EPS have distinct protein secondary structures. The
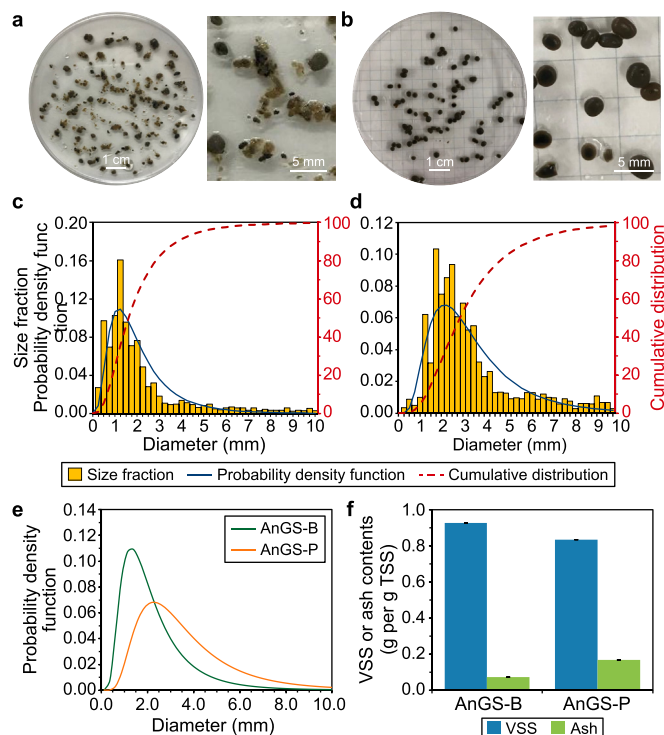

Fig. 2. a−b, Morphologies of anaerobic granular sludges and magnified view of bisected granules: AnGS-B (**a**) and AnGS-P (**b**). **c−d,** Particle size distribution of granular sludges based on diameters, including fractions, probability density function, and cumulative distribution: AnGS-B (**c**) and AnGS-P (**d**). **e,** Comparison between the lognormal distribution function of different granules. **f,** VSS and ash contents in original granular sludges.

Table 1

Average diameter and parameter values of lognormal distributions.

Sample	Average diameter (mm)	Lognormal distribution mean value	Lognormal distribution standard deviation
AnGS-B	2.3	0.552	0.637
AnGS-P	3.5	1.195	0.578
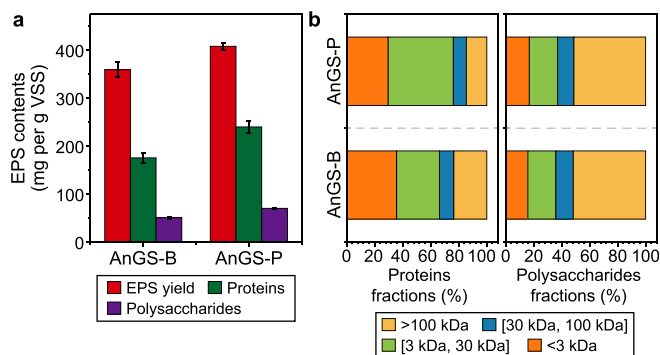
Fig. 3. a, EPS compositions. **b**, The distribution of proteins and polysaccharides in different size ranges.

Table 2

Variances of protein secondary structures in EPS extracts: second derivative and curve-fitted amide I region (1700−1600 cm^{-1}).

Secondary structures	AnGS-B	AnGS-P
β-sheet (1640−1630 cm^{-1})	35.91%	46.38%
β-turn (1680−1660 cm^{-1})	0.54%	0.40%
α-helix (1660−1650 cm^{-1})	29.86%	3.28%
random coil (1650−1640 cm^{-1})	33.69%	49.94%
(β-sheet + random coil)/α-helix	2.33	29.37

percentage distribution of each secondary structure in EPS is listed in Table 2. For EPS samples from AnGS-P, the fractions of β-sheet and random coil structure were over 96%, approaching 70% in AnGS-B. As reported, the value of (β-sheet + random coil)/α-helix was used to evaluate the compactness of the PN structure [30−32]. The higher the values, the looser the structure [33]. In summary, the extracted EPS is protein-rich and has a typical feature of the β-sheet structure; however, EPS contents and structure affected the functional groups of EPS derived from different granules.

Also, the chemical compositions of EPS were identified using the three-dimensional EEM spectroscopy technique. EEM spectra are used to identify the chemical properties of EPS, as fluorescence characteristics are strictly related to their structure and functional groups in molecules. Four main peaks were identified at the excitation/emission (Ex/Em) wavelength pairs of 220−230/340−350 nm (Peak A), 270−280/340−350 nm (Peak B), 330−350/420−450 nm (Peak C), and 260−270/430−440 nm (Peak D), respectively (Fig. 5). Two main peaks, A and B, were associated with protein-like products or aromatic amino acid tryptophan [15,34]. Peak A and Peak B with a high fluorescence intensity were identified in all samples, demonstrating that the tryptophan or PN-like components were the dominant substances in EPS contents. Also, differences were observed in Peaks C and D, which were only

identified in the AnGS-P sample. Peak C is related to humic acid-like organic matter [35]; Peak D is at 330−350/400−450 nm and is attributed to hydrophobic humic acid-like compounds.

3.4. Rheological behaviour reflecting strong similarities with gel materials

In Fig. 6a and b, the morphology of freeze-dried EPS products with different structures was visualised by SEM. The structure of AnGS-based EPS products was compact. Similarly, the EPS aqueous solution displayed distinctive rheological performance. EPS solutions with different fractions of 8−25% were studied in the following rheological tests.
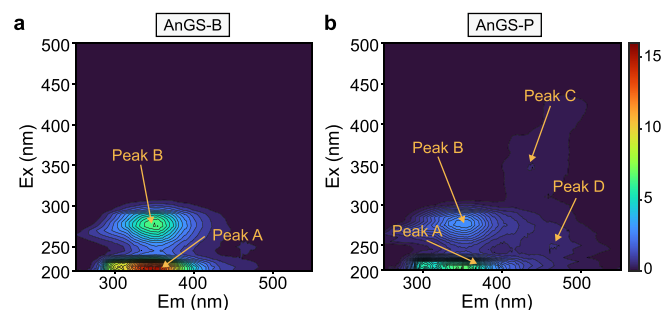

Fig. 5. Three dimensional-EEM fluorescence spectra of EPS extracts derived from different granular sludges: AnGS-B (**a**) and AnGS-P (**b**). The *x*-axis represents the emission spectra from 250 to 550 nm. In contrast, the *y*-axis is the excitation wavelength from 220 to 500 nm. 31 contour lines, as the third dimension, are shown for each EEM spectrum to represent the fluorescence intensity at an interval of 10 a. u.
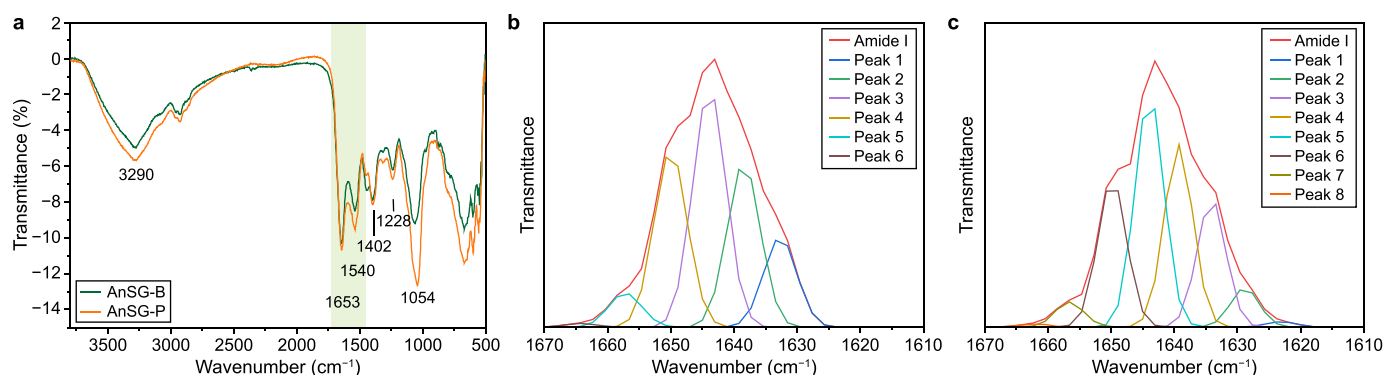

Fig. 4. a, ATR-FTIR spectra of EPS obtained from granular sludges. **b−c**, Second-derivative spectra for the amide I protein region: AnGS-B (**b**) and AnGS-P (**c**).

The rheological behaviour of biopolymers is closely associated with their design and optimisation for their downstream application. The evolution of storage (G′) and loss (G″) moduli is shown in Fig. 6c and d for all EPS aqueous suspensions in strain sweep measurements. Regardless of sludge types, G′ is almost constant at low shear strain values, suggesting a linear viscoelastic regime, in agreement with the results of activated sludges [36,37] and EPS solutions [38]. Moreover, since G′ > G″, the samples display a gel-like structure and can be defined as solid viscoelastic materials [39]. Beyond the LVE region and before reaching the flow point (i.e., G′ = G″), the samples enter a yielding region characterised by a reduction in their structural strength (reduction in G′) but still display a gel-like behaviour. Once the flow point is reached, the viscous component dominates (G″ > G′), and the samples start to flow. In this region, G′ and G″ both follow a power-law model typical of soft-glassy materials [37], also reported in many other systems such as activated sludges [37] and hydrogels [40]. Lastly, it is possible to notice that higher G′ values were obtained for more

concentrated EPS suspensions, suggesting that the gels' network strength and colloidal forces increased as a function of the EPS concentration [41].

Frequency sweep tests were performed at γ = 0.2% (i.e., the LVE limit) as a frequency function for all the EPS solutions investigated (Fig. 6e and f). All EPS samples display G′ > G″, with both moduli slightly increasing with the test frequency. In addition, the relatively large values of tan δ (=G″/G′ > 0.1, data not shown) suggest the typical behaviour of weak gels [42]. As expected, the viscoelastic parameters of the EPS solutions increase as a function of the EPS fractions, reflecting a more compact and dense structure associated with an increase in the solution's viscosity, as previously observed [38]. From this data, it is possible to extract the complex viscosity η* (Fig. 6g) of each specimen type at an oscillation frequency ν = 1 Hz. Observing the η* vs. EPS wt%, it is possible to note that the η* is nearly constant and in the range of a few tens/hundreds of Pa·s for AnGS-B samples. Conversely, for AnGS-P samples, a sharp increase of η* occurs at EPS concentrations higher than 15 wt% EPS, indicating the formation of a dense, extended 3D network above this concentration threshold [38]. This data, coupled with the information obtained from strain and frequency sweep tests, indicates different behaviour in the two specimens regarding viscoelastic properties.

3.5. Barrier properties of coated paper

The barrier properties were comprehensively investigated regarding the moisture and oil/grease resistance capacity of coated and uncoated paper (Fig. 7). Moisture resistance is one of the essential properties required for packaging materials with high moisture content. In Fig. 7a, the water absorbance capacities of CMC + EPS-coated paper were reduced by 49−65% compared to the blank and CMC samples, underlying less sensitivity to moisture and better water barrier performance compared with CMC-coated paper. The increased water-proof property was attributed to the more hydrophobic EPS layer. The EPS has been recognised as having many charged groups (e.g., carboxyl and hydroxyl groups) and polar groups (e.g., aromatics, aliphatics in PN, and hydrophobic regions in carbohydrates) [43]. The amphoteric character of the EPS depends on the presence of both hydrophilic and hydrophobic moieties, whose relative ratio is modulated by the composition of the EPS.

Interestingly, the water absorbance values of paper coated with EPS extracted from AnGS-P became the lowest, at 15.9 g m^{-2}, underlying better waterproofing performance than other materials. These differences may be associated with the presence of hydrophobic humic acid-like substances in the EPS and good rheological properties of EPS additives. Also, the enhanced waterproofing was positively related to the protein contents [44], whereas a weak correlation between PS and water absorbance was observed (Fig. 7c). These findings demonstrated that the water barrier properties should be associated with EPS rich in PN, and the coated PN for the AnGS-P sample were 4.7 g m^{-2}, 1.6 folds of the AnGS-B sample. According to the secondary structure of the protein (Section 3.3), higher values of (β-sheet + random coil)/α-helix in EPS extracted from the AnGS-P sample resulted in a looser structure of extracellular PN, which would help to expose the inner hydrophobic groups [30]. Furthermore, the functional groups in PS are mostly hydrophilic [30,45]. In this regard, a higher protein content facilitates the waterproofing performance of the coated paper by forming hydrophobic areas.

Meanwhile, the oil/grease resistance of EPS-based paper coatings was evaluated by a standard test (ISO 16532-1:2010). The time for turpentine oil to penetrate the CMC + EPS-based paper sheet was above 60 s, 2−8 times that for CMC-coated paper (30 s),
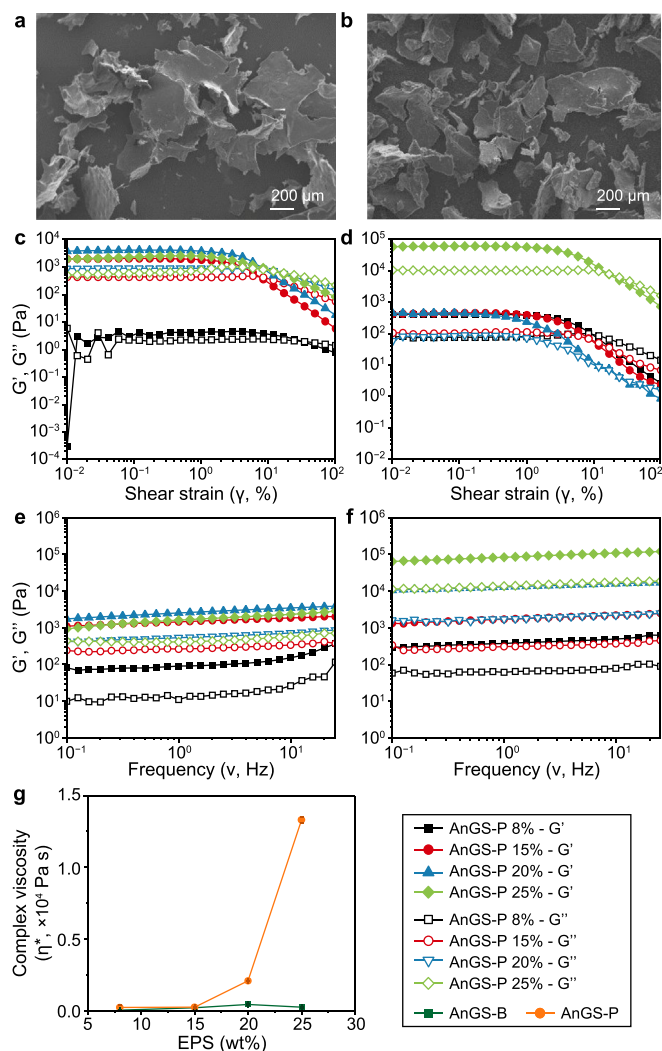

Fig. 6. a−b, SEM pictures for visualization of freeze-dried EPS extracts derived from two types of granular sludges: AnGS-B (**a**) and AnGS-P (**b**). **c−d**, Representative trend of storage (G′) and loss (G″) moduli resulting from strain sweep tests (γ = 0.01−100%) performed on EPS solutions at different weight concentrations (8−25 wt%) at T = 25 °C and γ = 0.2%: AnGS-B (**c**) and AnGS-P (**d**). **e−f**, Representative trend of G′ and G″ moduli of EPS solutions resulting from frequency sweep tests (ν = 0.01−100 Hz) performed at T = 25 °C and frequency = 1 Hz: AnGS-B (**e**) and AnGS-P (**f**). **g**, Complex viscosity (η*) as a function of the EPS concentration, in the 8−25 wt% range.
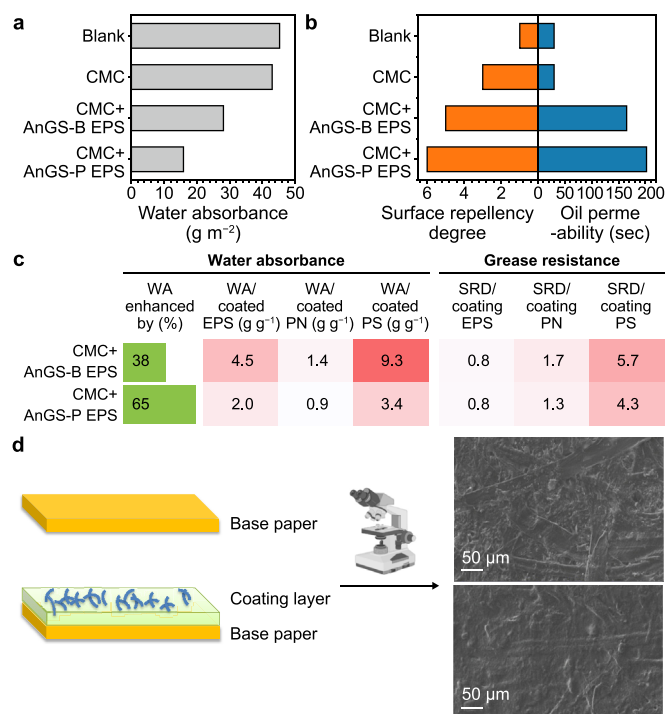
Fig. 7. a, Water absorption results based on the Cobb method. **b**, Oil and grease resistance of EPS multilayer coatings on raw paper sheets with the surface grease repellence based on the turpentine oil method (left panel); and permeability time needed for turpentine oil to penetrate the CMC and CMC + EPS coated paper sheets (right panel). Pristine paper sheets were used as the blank. **c**, The heatmap of water absorbed and grease resistance in the paper sheets standardised with coated EPS components. WA: water absorbance; SRD: surface repellency degree. **d**, A depiction of the multilayer concept for EPS and CMC coatings; SEM observation of the multilayer of composite films and coatings for active biodegradable packaging: Uncoated paper (Upper) and paper fabricated with AnGS-P EPS.

implying that adding EPS improved the paper's oil resistance (Fig. 7b). Similarly, the grease resistance effect exhibited by EPS was confirmed by an increase in the degree of grease surface repellence observed for the CMC + EPS-based paper (Fig. 7b). The values for the degree of grease repellence in other samples were 3−9, which were higher than the blank group (uncoated paper). However, some differences can be noted among the different materials. Similar to the water absorbance results, the degree of grease surface repellence for papers coated with the EPS samples of AnGS-P was better compared to other EPS additives.

SEM micrographs provide further insight into surface morphology: the paper's surface became smoother, more compact, and less porous after coating (Fig. 7d). These results implied that adding EPS resulted in a unique multilayer structure with improved water/grease resistance properties. That is to say, EPS coating was associated with modification of the fine structure of the paper's surface (i.e., becoming non-porous) and a higher fraction of hydrophobic contents in the EPS samples of AnGS-P. As suggested by others, forming a dense structure formed by fibrils results in high barrier properties [46]. Also, the conventional manner of combining CMC with other cellulose nanofibers showed a tendency to make a film on the paper's surface with a more uniform coverage [18]. CMC, an anionic derivative of cellulose that is prepared by introducing carboxymethyl groups along the cellulose chain, has been used in the papermaking industry as a surface sizing agent and coating binder due to the very good film making and water retention characteristic [47]. Interestingly, blending EPS with CMC resulted in an even higher improvement in barrier properties than

CMC-coated paper. Hence, this result is due to a dense and uniform coating structure on the paper surface that blocks pores. The hydrophilic characteristic of EPS is probably the main reason for this observation.

Based on the aforementioned findings, Fig. 7d illustrates the proposed hypothesis of using the mixture of EPS and CMC layers to enhance water, oil, and grease barrier performance. Multilayer structures are often used to boost functional performance over monolayer materials. With EPS coated on the raw paper, the structure of the paper was further manufactured to compromise two layers, i.e., the base and barrier layers. The barrier layer, namely the coating layer, is the outermost in the sandwich-like structure and is in direct contact with the external environment. In the barrier layer, EPS containing high extracellular PN rich in β-sheets and random coil PN would facilitate a structural role for paper coating. Under specific conditions, clusters of hydrophobic polypeptides would cover the surface, inducing phase separation of hydrophilic clusters within the CMC-containing bulk.

3.6. Significance of this work and implications for resource recovery of EPS derived from granular sludges

Wastewater contains substantial resources, ranging from 50% to 100% of lost waste resources [48]. Recovery of resources from wastewater (known as "water mining" or "wastewater biofactory") through product extraction is an emerging concept and becomes attractive for environmental protection, economy, and industrial areas. Different sources of granular sludge have distinctive EPS compositions closely associated with downstream applications of EPS-based biomaterials. Thus, in this study, a comprehensive evaluation of biomaterials' physicochemical properties, yield, and quality is significant for their potential application. Our findings of rheological behaviour reflecting strong similarities with gel materials can offer a vital theoretical basis for paper coating without additional modification. Interestingly, the paper coated with EPS of AnGS-P displayed a better waterproof or grease-resistance resistance, associated with modification of the fine structure of the paper's surface (i.e., becoming less-porous), and a higher fraction of hydrophobic contents in the EPS samples. EPS products separated from the AnGS-paper industry showed great potential for paper coating. EPS-based multilayer structures can be engineered by using automatic preparation for paper coating, which means that the EPS powder can be used as the input without any active reagents (e.g., CaCl$_2$), significantly enhancing the scalability of EPS products. Also, EPS derived from waste sludge holds great potential to be used as an alternative to commercial paper coating materials, contributing to carbon emissions reduction in the long term.

4. Conclusion

This work investigated the EPS properties of two distinct anaerobic granular sludges, advancing their potential application as paper coating materials. Regardless of the different sludge sources, EPS from both types were mainly composed of PN. EEM spectra confirmed that tryptophan or protein-like components were the dominant substances, together with humic-like components. The rheological behaviour test showed the strong similarity of EPS-based biomaterials to gel materials but different viscoelastic properties without any apparent link to the bioprocess catalysed by the pristine biomasses. The addition of EPS resulted in improved water/grease-proofing behaviour. The best results were achieved with the EPS samples from AnGS-P, characterised by a higher fraction of PN and hydrophobic contents than the other EPS samples. Moreover, the extracellular PN rich in β-sheets and random coil would facilitate a structural role for paper coating. Conclusively,

this research establishes for the first time that EPS derived from anaerobic granules exhibits interesting water barrier properties when used as paper coating additives. More importantly, from the paper industry's perspective, these EPS enhance resistance to grease penetration and absorbance. These biomaterials recovered from waste granular sludge provide a sustainable resource for industrial application and promise to realise a sustainable and circular economy.

CRediT authorship contribution statement

Cuijie Feng: Funding Acquisition, Conceptualization, Data Curation, Investigation, Methodology, Validation, Visualization, Writing - Original Draft, Writing - Review & Editing. **Lorenzo Bonetti:** Data Curation, Writing - Review & Editing. **Hui Lu:** Writing - Review & Editing. **Zhongbo Zhou:** Writing - Review & Editing. **Tommaso Lotti:** Writing - Review & Editing. **Mingsheng Jia:** Writing - Review & Editing. **Giacomo Rizzardi:** Methodology. **Luigi De Nardo:** Writing - Review & Editing. **Francesca Malpei:** Conceptualization, Supervision, Writing - Review & Editing.

Declaration of competing interest

The authors declare that they have no known competing financial interests or personal relationships that could have appeared to influence the work reported in this paper.

Acknowledgements

References

[1] S. de Valk, C. Feng, A.F. Khadem, J.B. van Lier, M.K. de Kreuk, Elucidating the microbial community associated with the protein preference of sludge-degrading worms, Environ. Technol. 40 (2) (2019) 192−201.

[2] M.C. van Loosdrecht, D. Brdjanovic, Anticipating the next century of wastewater treatment, Science 344 (6191) (2014) 1452−1453.

[3] K. van Leeuwen, E. de Vries, S. Koop, K. Roest, The energy & raw materials factory: role and potential contribution to the circular economy of The Netherlands, Environ. Manag. 61 (5) (2018) 786−795.

[4] C. Feng, L. Welles, X. Zhang, M. Pronk, D. de Graaff, M. van Loosdrecht, Stress-induced assays for polyphosphate quantification by uncoupling acetic acid uptake and anaerobic phosphorus release, Water Res. 169 (2020) 115228.

[5] C.d.A. de Carvalho, A.F. Dos Santos, T.J.T. Ferreira, V.N.S.A. Lira, A.R.M. Barros, A.B. Dos Santos, Resource recovery in aerobic granular sludge systems: is it feasible or still a long way to go? Chemosphere 274 (2021) 129881.

[6] C. Feng, T. Lotti, R. Canziani, Y. Lin, C. Tagliabue, F. Malpei, Extracellular biopolymers recovered as raw biomaterials from waste granular sludge and potential applications: a critical review, Sci. Total Environ. 753 (2021) 142051.

[7] N.K. Kim, N. Mao, R. Lin, D. Bhattacharyya, M.C. van Loosdrecht, Y. Lin, Flame retardant property of flax fabrics coated by extracellular polymeric substances recovered from both activated sludge and aerobic granular sludge, Water Res. 170 (2020) 115344.

[8] I. Tiseo, Production Volume of Paper and Paperboard 2010-2020, by Type, 2022.

[9] Y. Lin, K. Nierop, E. Girbal-Neuhauser, M. Adriaanse, M. Van Loosdrecht, Sustainable polysaccharide-based biomaterial recovered from waste aerobic granular sludge as a surface coating material, Sustainable Materials and Technologies 4 (2015) 24−29.

[10] Z.U. Arif, M.Y. Khalid, M.F. Sheikh, A. Zolfagharian, M. Bodaghi, Biopolymeric sustainable materials and their emerging applications, J. Environ. Chem. Eng. 10 (4) (2022) 108159.

[11] R. Hamza, A. Rabii, F.-z. Ezzahraoui, G. Morgan, O.T. Iorhemen, A review of the state of development of aerobic granular sludge technology over the last 20 years: full-scale applications and resource recovery, Case Studies in Chemical and Environmental Engineering 5 (2022) 100173.

[12] S.J. Lim, T.-H. Kim, Applicability and trends of anaerobic granular sludge treatment processes, Biomass Bioenergy 60 (2014) 189−202.

[13] APHA, Standard Methods for the Examination of Water and Waste Water, twenty-second ed., American Public Health Association, American Water Works Association, Water Environment Federation, 2012.

[14] O.G. Raabe, Particle size analysis utilizing grouped data and the log-normal distribution, J. Aerosol Sci. 2 (3) (1971) 289−303.

[15] C. Feng, T. Lotti, Y. Lin, F. Malpei, Extracellular polymeric substances extraction and recovery from anammox granules: evaluation of methods and protocol development, Chem. Eng. J. 374 (2019) 112−122, 2019.

[16] M. DuBois, K.A. Gilles, J.K. Hamilton, P.t. Rebers, F. Smith, Colorimetric method for determination of sugars and related substances, Anal. Chem. 28 (3) (1956) 350−356.

[17] P.K. Smith, R.I. Krohn, G. Hermanson, A. Mallia, F. Gartner, M. Provenzano, E. Fujimoto, N. Goeke, B. Olson, D. Klenk, Measurement of protein using bicinchoninic acid, Anal. Biochem. 150 (1) (1985) 76−85.

[18] S.M. Mazhari Mousavi, E. Afra, M. Tajvidi, D. Bousfield, M. Dehghani-Firouzabadi, Cellulose nanofiber/carboxymethyl cellulose blends as an efficient coating to improve the structure and barrier properties of paperboard, Cellulose 24 (2017) 3001−3014.

[19] Y. He, H. Li, X. Fei, L. Peng, Carboxymethyl cellulose/cellulose nanocrystals immobilized silver nanoparticles as an effective coating to improve barrier and antibacterial properties of paper for food packaging applications, Carbohydr. Polym. 252 (2021) 117156.

[20] D. Batstone, J. Keller, Variation of bulk properties of anaerobic granules with wastewater type, Water Res. 35 (7) (2001) 1723−1729.

[21] T. Lotti, E. Carretti, D. Berti, M.R. Martina, C. Lubello, F. Malpei, Extraction, recovery and characterization of structural extracellular polymeric substances from anammox granular sludge, J. Environ. Manag. 236 (2019) 649−656.

[22] A.G. Geyik, B. Kılıç, F. Çeçen, Extracellular polymeric substances (EPS) and surface properties of activated sludges: effect of organic carbon sources, Environ. Sci. Pollut. Res. 23 (2) (2016) 1653−1663.

[23] Y.-Q. Liu, J.-H. Tay, Fast formation of aerobic granules by combining strong hydraulic selection pressure with overstressed organic loading rate, Water Res. 80 (2015) 256−266.

[24] S. Sun, X. Liu, B. Ma, C. Wan, D.-J. Lee, The role of autoinducer-2 in aerobic granulation using alternating feed loadings strategy, Bioresour. Technol. 201 (2016) 58−64.

[25] Y. Ji, X. Yang, Z. Ji, L. Zhu, N. Ma, D. Chen, X. Jia, J. Tang, Y. Cao, DFT-calculated IR spectrum amide I, II, and III band contributions of N-methylacetamide fine components, ACS Omega 5 (15) (2020) 8572−8578.

[26] L. Zhu, H.-y. Qi, Y. Kong, Y.-w. Yu, X.-y. Xu, Component analysis of extracellular polymeric substances (EPS) during aerobic sludge granulation using FTIR and 3D-EEM technologies, Bioresour. Technol. 124 (2012) 455−459.

[27] X. Guo, X. Wang, J. Liu, Composition analysis of fractions of extracellular polymeric substances from an activated sludge culture and identification of dominant forces affecting microbial aggregation, Sci. Rep. 6 (1) (2016) 1−9.

[28] Y. Lin, C. Reino, J. Carrera, J. Pérez, M.C. van Loosdrecht, Glycosylated amyloid-like proteins in the structural extracellular polymers of aerobic granular sludge enriched with ammonium-oxidizing bacteria, Microbiologyopen 7 (6) (2018) e00616.

[29] A. Barth, Infrared spectroscopy of proteins, Biochim. Biophys. Acta Bioenerg. 1767 (9) (2007) 1073−1101.

[30] X. Hou, S. Liu, Z. Zhang, Role of extracellular polymeric substance in determining the high aggregation ability of anammox sludge, Water Res. 75 (2015) 51−62.

[31] E. Li, Y. Wang, D. Zhang, X. Fan, Z. Han, F. Yu, Siderite/PMS conditioning-pressurized vertical electro-osmotic dewatering process for activated sludge volume reduction: evolution of protein secondary structure and typical amino acid in EPS, Water Res. 201 (2021) 117352.

[32] C. Yin, F. Meng, G.-H. Chen, Spectroscopic characterization of extracellular polymeric substances from a mixed culture dominated by ammonia-oxidizing bacteria, Water Res. 68 (2015) 740−749.

[33] W. Wang, Y. Yan, J. Wang, J. Zhu, J. Ma, Z. Jiang, Y. Wang, Comparison and optimization of extraction methods of extracellular polymeric substances in anammox granules: from maintaining protein secondary structure perspective, Chemosphere 259 (2020) 127539.

[34] W. Wang, D. Li, S. Li, H. Zeng, J. Zhang, Characteristics and formation mechanism of hollow Anammox granular sludge in low-strength ammonia sewage treatment, Chem. Eng. J. 421 (2021) 127766.

[35] W. Chen, P. Westerhoff, J.A. Leenheer, K. Booksh, Fluorescence excitation-emission matrix regional integration to quantify spectra for dissolved organic matter, Environ. Sci. Technol. 37 (24) (2003) 5701−5710.

[36] H.-F. Wang, Y.-J. Ma, H.-J. Wang, H. Hu, H.-Y. Yang, R.J. Zeng, Applying rheological analysis to better understand the mechanism of acid conditioning on activated sludge dewatering, Water Res. 122 (2017) 398−406.

[37] J.-C. Baudez, R.K. Gupta, N. Eshtiaghi, P. Slatter, The viscoelastic behaviour of raw and anaerobic digested sludge: strong similarities with soft-glassy materials, Water Res. 47 (1) (2013) 173−180.

[38] T. Lotti, E. Carretti, D. Berti, C. Montis, S. Del Buffa, C. Lubello, C. Feng, F. Malpei, Hydrogels formed by anammox extracellular polymeric substances: structural and mechanical insights, Sci. Rep. 9 (1) (2019) 1−9.

[39] M.C. Tanzi, S. Farè, Characterization of Polymeric Biomaterials, Woodhead Publishing, 2017.

[40] H.M. Shewan, J.R. Stokes, Review of techniques to manufacture micro-hydrogel particles for the food industry and their applications, J. Food Eng. 119 (4) (2013) 781−792.

[41] R. Glicklis, L. Shapiro, R. Agbaria, J.C. Merchuk, S. Cohen, Hepatocyte behavior within three-dimensional porous alginate scaffolds, Biotechnol. Bioeng. 67 (3) (2000) 344−353.

[42] C.S. Hundschell, A.M. Wagemans, Rheology of common uncharged exopoly-saccharides for food applications, Curr. Opin. Food Sci. 27 (2019) 1−7.

[43] H.-C. Flemming, J. Wingender, The biofilm matrix, Nat. Rev. Microbiol. 8 (9) (2010) 623.

[44] P. Tyagi, L.A. Lucia, M.A. Hubbe, L. Pal, Nanocellulose-based multilayer barrier coatings for gas, oil, and grease resistance, Carbohydr. Polym. 206 (2019) 281−288.

[45] X. Wang, H. Yang, Y. Su, X. Liu, J. Wang, Characteristics of anammox granular sludge using color differentiation, and nitrogen removal performance of its immobilized fillers based on microbial succession, Bioresour. Technol. 333 (2021) 125188.

[46] H. Yousefi, M. Faezipour, S. Hedjazi, M.M. Mousavi, Y. Azusa, A.H. Heidari, Comparative study of paper and nanopaper properties prepared from bacterial cellulose nanofibers and fibers/ground cellulose nanofibers of canola straw, Ind. Crop. Prod. 43 (2013) 732−737.

[47] M. Blomstedt, Modification of Cellulosic Fibers by Carboxymethyl Cellulose: Effects on Fiber and Sheet Properties, Helsinki University of Technology, 2007.

[48] D. Puyol, D.J. Batstone, T. Hülsen, S. Astals, M. Peces, J.O. Krömer, Resource recovery from wastewater by biological technologies: opportunities, challenges, and prospects, Front. Microbiol. 7 (2017) 2106.